Experimental Thermal and Fluid Science 99 (2018) 190–199

Contents lists available at ScienceDirect

Experimental Thermal and Fluid Science

journal homepage: www.elsevier.com/locate/etfs

Active heat sink with piezoelectric translational agitators, piezoelectric synthetic jets, and micro pin fin arrays

Taiho Yeom[a,b], Terrence Simon[b], Min Zhang[b,c], Youmin Yu[b], Tianhong Cui[b,*]

[a] Department of Mechanical Engineering, University of Mississippi, University, MS 38677, USA
[b] Department of Mechanical Engineering, University of Minnesota, Minneapolis, MN 55455, USA
[c] Graduate School at Shenzhen, Tsinghua University, Shenzhen 518055, China

ARTICLE INFO

Keywords:
Active heat sink
Thermal management
Piezo fan
Synthetic jet
Micro pin fin
Surface microstructure
Electronics cooling
Piezoelectric
Actuator

ABSTRACT

Air-cooled heat sinks are widely used for electronics cooling. Active and passive cooling components can be added to enhance the performance of the air-cooled heat sinks. In this paper, piezoelectric translational agitators and synthetic jets are integrated as active cooling components while micro pin fins are adopted as a passive cooling scheme. The heat transfer performance of the active heat sink system that combines these active and passive cooling components along with a suction fan is experimentally investigated. The piezoelectric translational agitators installed within cooling channels are operating at 222 Hz ~ 820 Hz with a peak-to-peak displacement of 1.0 mm ~ 1.4 mm, depending on the attached carbon fiber blade type. The piezoelectric synthetic jet array provides impingement flow into the cooling channels with an inclined configuration, that has been successfully integrated into the system without interference with other components by using a wedge platform. The jet operates at 720 Hz with the jet velocity of up to 39 m/s. Micro pin fins are fabricated onto both surfaces of each heat sink channel walls by a double-sided microfabrication technique. They have diameter, height, and spacing of 500 μm, 250 μm, and 1500 μm, respectively. The experimental results indicate that the micro pin fins are most efficient among the employed active and passive cooling components, reducing thermal resistance up to 38%, compared to plain heat sink performance. The piezoelectric translational agitator reduces system thermal resistance by 22%, compared to the non-agitated condition, at the same through-flow rate. The synthetic jet shows weaker cooling capability in the setting tested, compared to enhancement by the agitator plates or pin fins. The active heat sink with the micro pin fins, agitators, and jets provides a thermal resistance of 0.064 °C/W at 70 CFM (33 L/sec) through-flow of air, about a 48% reduction from that of the non-agitated, plain heat sink under the same operating conditions. The results demonstrate how more effective the active heat sink system is compared to traditional air-cooled heat sinks.

1. Introduction

Increasing heat dissipation of modern power electronics drives continuous development of a variety of passive and active cooling technologies using air, water, and other non-conductive liquids, as coolants. Liquid cooling, such as single-phase [1,2], direct spray [3–7], microchannel geometries [8–10], and boiling heat transfer [11–18], can provide substantial cooling capability. However, liquid cooling adds considerable cost, weight, volume, and complexity to complete an entire cooling loop, such as pumps, pipes, hoses, reservoirs, nozzles, and orifices. Reliability is another issue as leakage, condensation, and corrosion can cause critical failures to electronics. On the other hand, air possesses many advantages over liquid cooling due to its inherent characteristics. For instances, it is more reliable, cost effective, and environmentally favorable. Therefore, though cooling with air-using traditional methods is less effective than liquid cooling, there is still strong motivation for further advancing air cooling to maximize its capability. A traditional air cooling technique for electronics is the combination of fins and an external blower that can generate forced air flow through channels between fins. However, the blower-aided heat sink system is continuously challenged by rising system heat fluxes with each generation of electronics, and requires increasing cooling capability to meet elevating heat removal needs. To address, without moving to liquid cooling, one can consider incorporating active and passive cooling components into a blower-driven heat sink system. Effective active components disturb thermal boundary layers to enhance surface heat transfer beyond those in simple channel flows. Many active air cooling techniques have been developed, either as a stand-alone or

* Corresponding author.
E-mail address: cuixx006@me.umn.edu (T. Cui).

https://doi.org/10.1016/j.expthermflusci.2018.07.035
Received 24 February 2018; Received in revised form 22 June 2018; Accepted 28 July 2018
Available online 30 July 2018

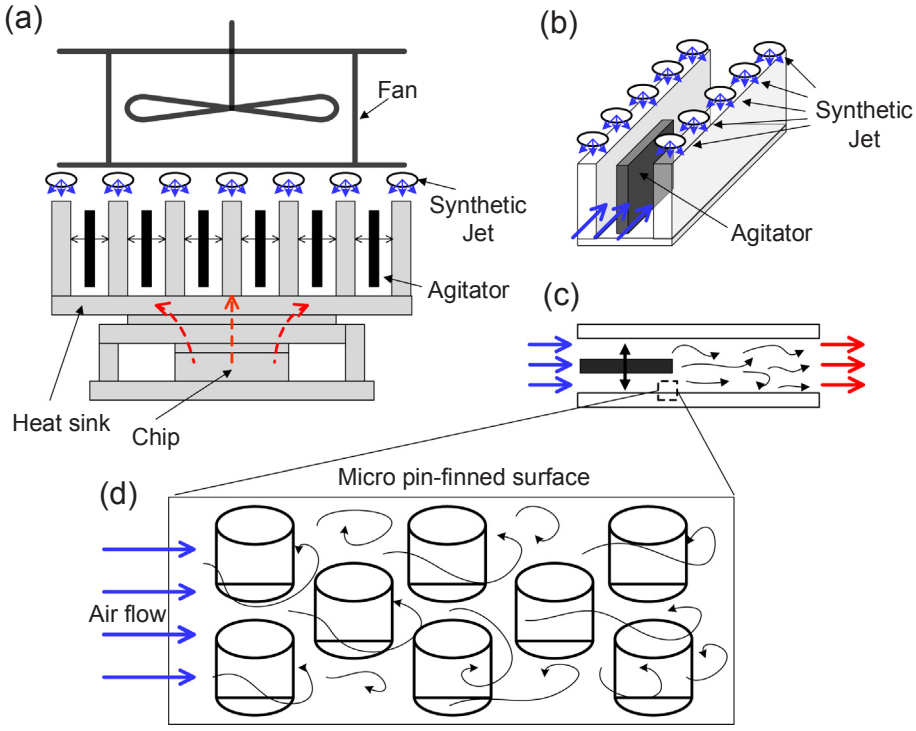

Fig. 1. Conceptual schematic of proposed active heat sink system with translational agitators, synthetic jets, and micro pin fin arrays; (a) Active heat sink; (b) Single channel configuration with synthetic jet arrays and agitator; (c) Flow behavior in the active heat sink channel with an oscillating short agitator blade; (d) Micro pin fin arrays on the heat sink channel surfaces.

as added devices, to air-cooled heat sink systems. A piezoelectric fan is one of them. Bi- or mono-morph piezoelectric ceramic layers resonate attached flexible blades, yielding flapping motion from the tips of the blades. Air currents from the flapping tips are used to cool heated surfaces. Since Toda and Osaka [19] proposed the concept of a piezoelectric fan, extensive studies have been conducted to understand and optimize their characteristics. Yoo et al. [20] investigated vibration characteristics of a piezoelectric fan operating at 60 Hz with a maximum peak-to-peak displacement of 35.5 mm. The applied voltage was 220 V. The size of the fans ranged from 28.6 mm to 69 mm. Açikalin et al. [21] studied thermal performance of piezoelectric fans in a small portable electronics environment with various overlapping displacements and mounting configurations relative to the heat sink. The length of one fan was 63.5 mm and its resonance frequency was 20 Hz. The fan generated a peak-to-peak displacement of 15 mm. The results show that the half-overlapped and horizontally-positioned fan provided the largest heat transfer coefficient of 102 W/m^2 K. Wait et al. [22] investigated via numerical and experimental methods piezoelectric fans operating under higher resonance modes. They concluded that the second resonance mode generated the best thermal performance, while exhibiting the largest power consumption. Recently, there have been attempts to incorporate piezoelectric fans in heat sink channels. Ma et al. [23] analyzed the effects of operating frequency, displacement, fan arrangement, and power consumption in a heat sink channel made of aluminum. The optimum system showed that the dimensionless PZT-convection number, the ratio between the PZT convection to heat sink natural convection, reached 2.3. Sufian and Abdullah [24] conducted experimental and numerical studies on a finned heat sink with vertically inserted piezoelectric fans used as a high-power LED cooling system. Quadruple piezoelectric fans improved thermal performance of the heat sink system by 3.8 times. Yeom et al. [25] proposed a piezoelectric agitator that can generate translational movement to blades embedded in heat sink channels. In a single channel experiment, the agitator, coupled with a channel flow, improved heat transfer by 55%, compared to a channel-flow only forced convection. Another type of active cooling technique is a piezoelectric synthetic jet. A diaphragm attached to one side of a cavity oscillates, driven by a piezoelectric patch, generating a train of vortex rings emerging from an orifice on the opposite side. Beratlis and Smith [26] performed a numerical optimization study of synthetic jets as cooling devices for laser arrays. Mahalingam et al. [27] developed a piezoelectric synthetic jet ejector that can generate secondary flow in the heat sink channel. The heat sink combined with the synthetic jet ejector achieved 350% enhancement in heat transfer, compared to natural convection values. Arik [28] investigated the localized heat transfer performance of a piezoelectric synthetic jet driven at a resonance frequency of between 2000 Hz and 6000 Hz. Over a heater of 6.25 mm length, the synthetic jet enhanced thermal performance by 10 times, compared to natural convection. Passive cooling, such as micro pin-finned surfaces, can bring significant contributions in enhanced heat transfer performance to a heat sink system. Marques and Kelly [29] achieved up to 450% heat transfer enhancement using a nickel micro pin fin heat exchanger with cross flow of air. Wang et al. [30] performed an experimental study to understand thermal and hydraulic mechanisms of a single micro pillar in a microchannel with different cross-sectional shapes. The microchannel with a micro pillar provided a heat transfer coefficient that was two times that of the plain microchannel. Among the different cross-sectional shapes; circular, triangular and diamond, the triangular pillar showed the best thermal performance. Much effort has been made to optimize on pin-fin geometry, size, spacing, array configuration, and materials [31–35]. Most of these studies were done in mini or microchannel conditions. Yeom et al. [36] conducted an experimental study on heat transfer and pressure drop characteristics of micro pin fin arrays in an air-flow channel under both laminar and turbulent flow regimes. The maximum heat transfer enhancement of 79% was achieved over plain surfaces due to the micro pin fin arrays that had a height of 250 μm and a diameter of 400 μm. The array configuration was staggered. Yeom et al. [37] introduced an active heat sink system combined with a piezoelectric translational agitator and micro pin fin arrays. The full-size heat sink with 26 channels aided by the agitator and micro pin fins decreased the system thermal resistance to 0.065 °C/W. This was a 45% reduction in thermal resistance, compared to that of a heat sink system with plain surfaces and no agitation. The current paper extends the previous study on active heat sink technology by Yeom et al. [37], combining the piezoelectric translational agitators, piezoelectric synthetic jets, and micro pin fins to maximize the heat transfer

performance of an active heat sink system. The purpose of the study is to demonstrate that the active heat sink system combined with active and passive cooling devices can provide exceptional cooling performance, compared to that of conventional fan-assisted heat sinks. The component-level studies can be found in the previous work [25,36–40] that shows the effects of various parameters used in the current study on heat transfer and pressure drop performances.

2. Active heat sink system

Fig. 1 shows a conceptual schematic of the active heat sink system under study. It combines translational agitators, synthetic jets, and micro pin fin arrays. In a traditional fan-assisted heat sink system, heat from the chip transfers through interface materials to the heat sink. The air flow through the heat sink channels generated by the fan carry away heat to the ambient. Components embedded within the channels can disturb the thermal boundary layers to enhance heat transfer. The main objective of the proposed design is to provide active cooling effects throughout the entire flow path of heat sink channels. The translational agitator blades (Fig. 1(a) and (b)) oscillating within the channels disturb the thermal boundary layers formed on the sides and bottom surface of the channels. The synthetic jet arrays (Fig. 1(b)) impinge air vortex rings onto the tips of the heat sink fins and into the channels they form. Ideally, the agitators and synthetic jets cover the entire exposed surfaces of the heat sink channels, providing strong agitation effects. In addition, the micro pin fins (Fig. 1(d)) on the side surfaces of the channels increase heat transfer area and further disturb the flow. The agitator blades can be either short or long (extending over a portion of the channel, as shown in Fig. 1(c)). The long blades can directly disturb the thermal boundary layers on the wall mostly by strong pressure gradients, while the short blades generate vortices at their trailing edges that can enhance convective heat transfer downstream in the channel.

2.1. Heat sink design

The proposed heat sink is shown in Fig. 2. It has 26 channels formed by an array of 27 fins made out of copper. The base of the heat sink has an area of 114 mm × 89 mm (4.5 in. × 3.5 in.). The fin thickness and height are 1.1 mm and 23.6 mm, respectively. The heat sink is designed to couple with an induced flow fan. The air enters from both sides of each channel, and discharges upward in the center to the fan inlet. The heat sink has four arrays of slots through the fins to accommodate frames used for driving agitator blades. Each fin was cut by wire Electrical Discharge Machining (EDM), and soldered to the heat sink base.

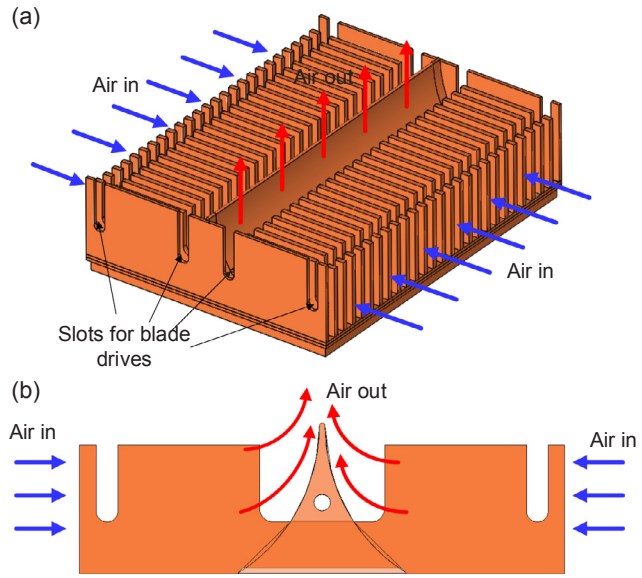

Fig. 2. (a) Copper heat sink with 26 channels, (b) channel cross sectional view with air flow directions.

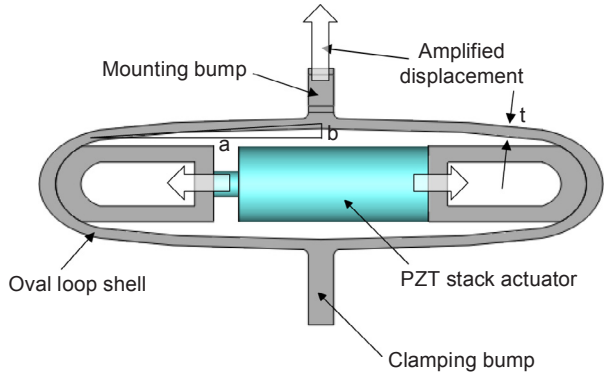

Fig. 3. Oval loop shell piezoelectric actuator.

2.2. Piezoelectric translational agitator

Translational agitation is realized using a resonance energy of an oval loop shell excited by a PZT stack. Yeom et al. [38] conducted a detailed study on structural and dynamic characteristics of the oval loop shell actuator shown in Fig. 3. The PZT stack actuator is located in the center of the loop, and is connected to the oval loop shell through two small connector pieces at the sides. The PZT stack generally produces a very small displacement, about 0.1% of its length, in the actuation direction. The oval loop shell actuator amplifies this small displacement changing its actuation direction from horizontal to perpendicular as shown in Fig. 3. When the operating frequency of the PZT stack approaches the natural frequency of the oval loop shell, the amplified displacements are maximized by resonance energy. At the first resonance mode, the lower beam of the shell structure is excited, moving the entire actuator body in the vertical direction, which is orthogonal to the longitudinal direction of the PZT stack. At the second resonance mode, only the upper beam is excited, generating high frequency and large displacement translational actuation without moving the entire actuator body. In this study, we used the second resonance mode to generate strong air currents from blade structures attached to the oval loop shell actuator. The performance of the actuator is characterized by the three key parameters, a, b, and t, shown in Fig. 3. The values of a, b, and t are 40.0 mm, 1.8 mm, and 1.6 mm, respectively. The width of the shell is 8.0 mm. The resonance frequency of the actuator at the second mode is 921 kHz.

In the current study, several agitators were fabricated to demonstrate the thermal performance of the active heat sink system. Fig. 4 shows piezoelectric translational agitators (PTA-1, PTA-2, and PTA-3) with three different types of blade structure. Carbon fiber composite plates were used to fabricate the blade structures. They have very high stiffness-to-weight ratios, ensuring high resonance frequencies of the agitators, compared to other common metal or plastic materials. The blade structures were designed in a way that the driving rods go through in the middle of the blade plates. This is to ensure high stiffness and to prevent any asymmetric flapping motions of the blade structures. The blades and driving rods were cut by a water jet, and assembled using epoxy in a specially fabricated mold to ensure tight dimensions and tolerances. The vibration and dynamics characteristics of the agitators were investigated by a scanning Laser Doppler Vibrometer (LDV) system.

PTA-1 has 26 long agitator blades that occupy the entire channel length. It is driven by the single oval loop shell actuator. The operating

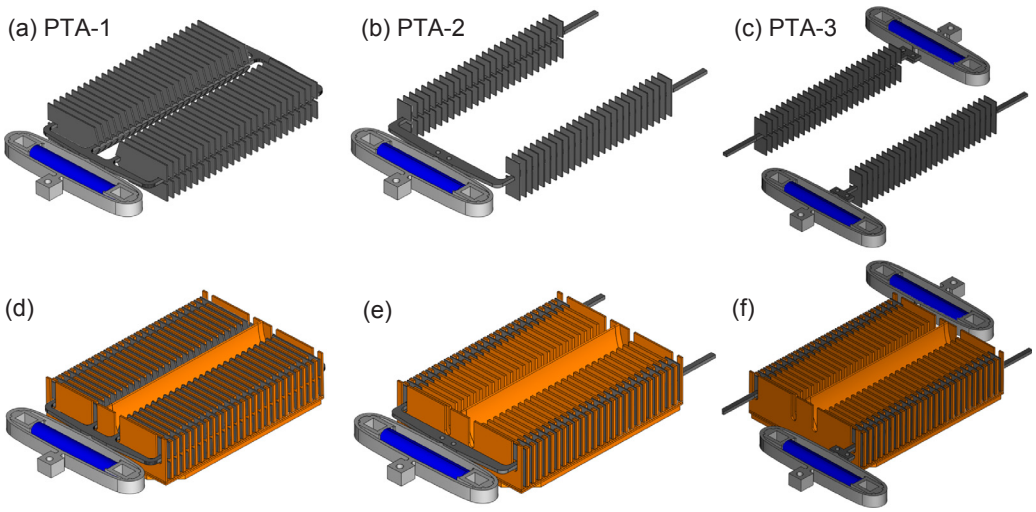

Fig. 4. Piezoelectric translational agitators with carbon fiber blade structures: (a) PTA-1: long blade structure with one actuator, (b) PTA-2: short blade with one actuator, (c) PTA-3: short blade with two actuators, (d) PTA-1 installed in the heat sink, (e) PTA-2 installed in the heat sink, (f) PTA-3 installed in the heat sink.

Table 1
Operating conditions of the piezoelectric translational agitators.

Agitator type	Blade weight (g)	Operating frequency (Hz)	Power consumption (W)	Peak-to-peak displacement (mm)
PTA-1	37.0	222	2.5	1.0
PTA-2	11.5	512	5.0	1.4
PTA-3	5.5 (each)	780, 820	5.6 (each)	1.4

frequency is 222 Hz, and the peak to peak displacement is 1.0 mm. PTA-2 and PTA-3 have short blades that oscillate within the upstream portion of the channel. These are driven by the same actuator as listed with PTA-1. The operating frequencies of PTA-2 and PTA-3 are higher than that of PTA-1 due to decreased weight of the blade structures. PTA-2 operates at 512 Hz. Two PTA-3 agitators show different operating frequencies of 780 Hz and 820 Hz due to their fabrication variability. The peak to peak displacement is 1.4 mm. The operating conditions of the piezoelectric translational agitators are summarized in Table 1. The power consumption values of the agitators, measured under ambient conditions, are 2.5 W, 5.0 W and 5.6 W for PTA-1, PTA-2 and PTA-3, respectively at a driving voltage of 140 V. Fig. 4(d), (e), and (f) shows the agitators installed in the heat sink. The detailed performance evaluations of the translational agitator, based on dimensionless numbers, Reynolds number and Stanton number, in a single-channel environment were presented in the previous work [25].

2.3. Piezoelectric synthetic jet

A piezoelectric synthetic jet is another active cooling component added to the active heat sink system. One of the challenges in designing the active heat sink system is to avoid interferences between components of the system. The synthetic jet with a wedge platform can be a solution. Fig. 5 shows the proposed piezoelectric synthetic jet module with the wedge platform. A single oval loop shell actuator is used to drive the piston of the jet attached to the cavity on the inclined surface of the wedge platform. The cavity is sealed with a latex sheet. There are 25 arrays of orifices, and each array has four orifices aligned with a staggered configuration along the heat sink fins, making the orifice flows wall jets. The cavity and orifices are connected through inclined channels in the wedge platform. The cavity depth is 10 mm with an area of 30 mm × 100 mm. The orifice has a square shape of 0.9 mm × 0.9 mm. The operating frequency of the jets is 720 Hz at 180 V. The required electrical power to drive a single synthetic jet array with the above operating conditions is about 4.0 W. An inherent penalty of the jet system is tied to flow losses in the long flow passage channel that connects the cavity and orifices. Ayaskanta et al. [40] conducted a numerical and experimental study to optimize the wedge jet configuration in terms of orifice size and length of the jet flow path. The optimization result led to the configuration of the inclined jet system having a 2.5 mm diameter circular orifice with a jet inclined angle of 62 degrees from the horizontal plane. More details about the optimization work on the inclined jet configurations can be found in the previous work [40]. The present piezoelectric synthetic jet uses the recommendations of this study. The measured jet velocities of the inclined synthetic jet range from 31 m/s to 39 m/s.

2.4. Micro pin fins

Micro pin fins can significantly increase convective heat transfer area, and help disturb thermal boundary layers of the heat sink channel surfaces. Some of the key findings from the previous study by Yeom et al. [36] on micro pin fins tested in a single channel without oscillating plate agitation are as follows. First, fluid dynamic effects caused by the micro pin fins can play an important role in heat transfer improvement, and may exceed the effects of mere area increase. Second, the fluid dynamics effects become stronger with increasing pin fin diameter when the height is fixed. Third, the micro pin fins of 250 μm height and 400 μm diameter show the largest heat transfer performance among eleven fabricated micro pin fin configurations tested. Their pitch-to-diameter ratio is 3. Based on these previous observations, the micro pin fin employed in the current study has a diameter, height, and pitch of 500, 250, and 1500 μm, respectively. The diameter is increased by 100 μm from the best configuration of the previous study to account for the increased heat sink channel width and agitator blade displacement. These fins have been shown to improve heat transfer performance, based on this previous study [36]. The micro pin fins are configured in a staggered pattern. A double-sided microfabrication process was utilized to make the fins on a copper substrate, which was then cut into individual heat sink fins. The fabrication process of the heat sink channels with micro pin fins is as follows: A circular copper substrate 102 mm in diameter and 1.1 mm thick was preprocessed after cleaning with acetone, methanol, isopropyl alcohol, potassium hydroxide, and sulfuric acid. A titanium (Ti) layer was deposited on the both sides of the substrate as an adhesive layer. Next, KMPR photoresist was coated on the Ti layers on both sides. The KMPR layers were exposed to UV light and patterned to develop a mold structure for electroplating the

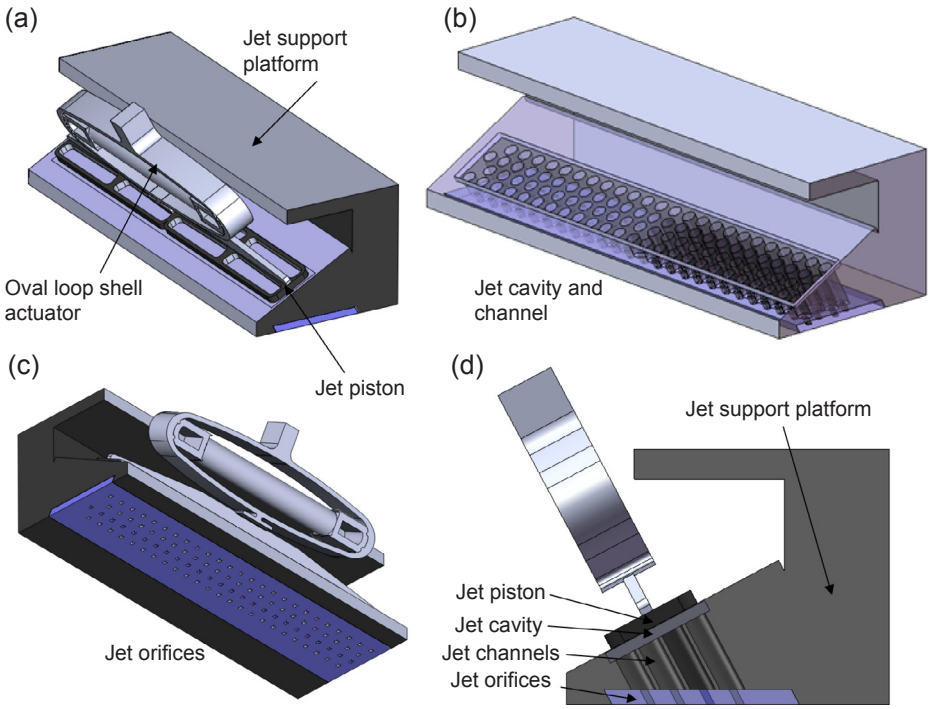

Fig. 5. (a) Piezoelectric synthetic jet module with a wedge platform, (b) jet cavity and channels on the wedge platform, (c) jet orifices, (d) cross section of the jet system.

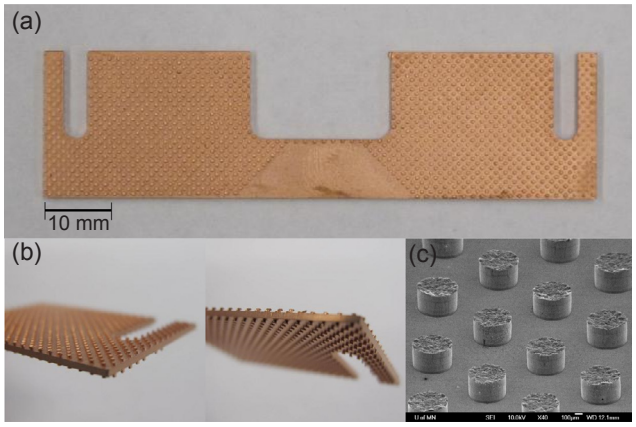

Fig. 6. (a) Single copper heat sink fin cut by wire EDM, (b) micro pin fins electroplated on the surfaces of the heat sink fin, (c) SEM image of micro pin fins.

micro pin fins on the substrate. The Ti layers were etched away in the patterned areas using diluted hydrofluoric acid. As a next step, copper micro pin fins were electroplated over the patterned substrate in a plating bath. Finally, the residuals of KMPR and Ti layers were removed to obtain a double-sided micro pin-finned plate. The copper plates with electroplated micro pin fins were cut into the heat sink fin shape using wire EDM. A heat sink fin with electroplated micro pin fins is shown in Fig. 6.

2.5. Assembly of active heat sink

Fig. 7 shows a snapshot of the actual active heat sink assembly with a suction fan, two PTA-3 agitators, and two synthetic jet arrays on their wedge platforms. The assemblies of inclined synthetic jet modules with the oval loop shell actuators are attached on the top of the heat sink base leaving space in the center for air flow from the heat sink discharge outlet to the inlet of the fan. The jet orifices are aligned to the upstream of the heat sink fins in staggered configuration to create a wall jet configuration. Additional fixtures to support the agitator and jet structures are not shown in the figure, for simplicity.

3. Heat transfer experiments

Previous studies on heat transfer performance of micro pin fins under translational agitation conducted in a single channel were presented [39]. Based on the single channel experimental results with micro pin fins and agitation combined, estimated system thermal resistance, calculated for the current heat sink (but without synthetic jets) was about 0.04 °C/W. This is considered to be good thermal performance, compared to commercially available fan-assisted heat sinks with typical thermal resistance values of 0.1 ~ 1.0 °C/W. However, this represents an ideal condition that eliminates several limitations of the actual system. As measured, the actual active heat sink system shows a higher thermal resistance of 0.065 °C/W [37]. This is mainly due to loss in the actual heat sink of some heat transfer area because the agitator driving rods pass through the heat sink fins, reducing heat transfer area. Also, the actual system tested may have leakage around heat transfer surfaces. In the current study, the heat transfer performance of the full-size actual system is measured that combines all the effects of agitators, jets, and micro pin fins.

3.1. Heat transfer experiment set up

The heat transfer experiments were performed with the active heat sink system shown in Fig. 7, except that the suction fan was replaced with a discharge adaptor connected to an external vacuum pump to easily manipulate and measure the volumetric flow rate through the heat sink. This allows separation of the fan head and flow characteristics from the heat sink pressure drop characteristics. For the external vacuum pump, a commercially available wet/dry vacuum cleaner (Dayton 4YE58) was used to provide the flow rate to the system. Fig. 8 shows the test section of the active heat sink for the heat transfer experiments. At the bottom, a glass fiber insulation layer is positioned to block heat loss to the ground. Next, a heat spreader in which ten

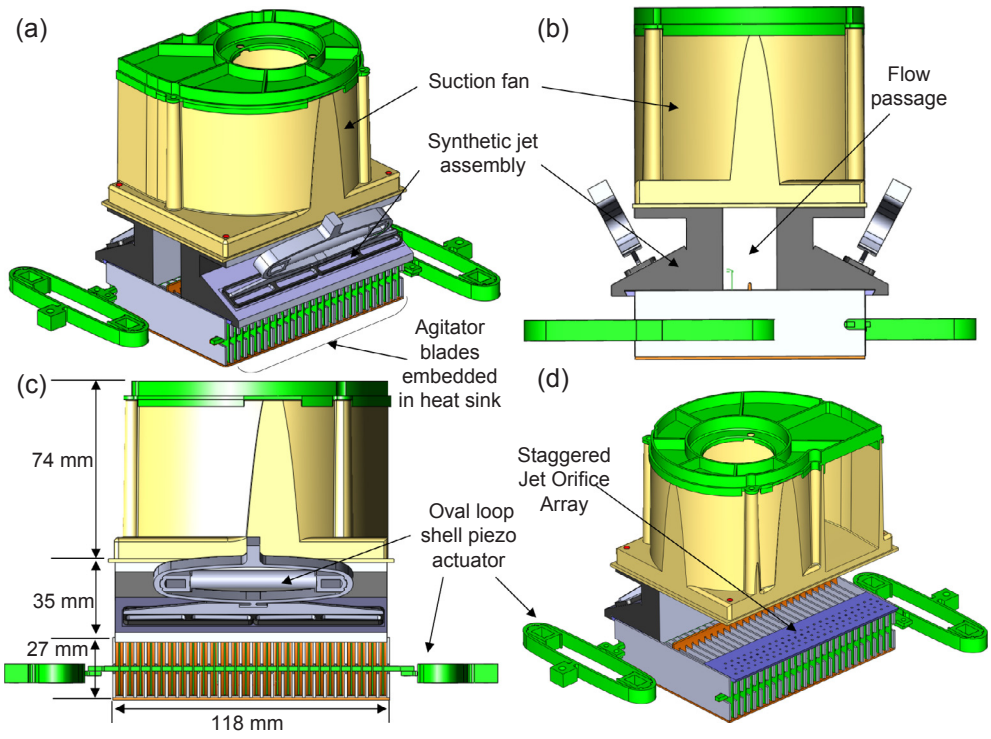

Fig. 7. Assembly of active heat sink system with a suction fan installed on the top.

cartridge heaters are inserted supports the active heat sink module. A high-conductivity thermal paste is used between the heat spreader and the heat sink to ensure minimal thermal contact resistance. Air temperatures are measured using thermocouples at the inlets and in the middle of the flow discharge adaptor at the outlet. The tests are done at the ambient condition of 300 K and 1 atm. A pressure tap is located at the outlet of the heat sink to obtain pressure drop across the heat sink system. The heat sink base temperatures are measured at different locations of the base, including the bottom and side surfaces. Then, the temperatures are averaged to calculate the system thermal resistance, R_{th}:

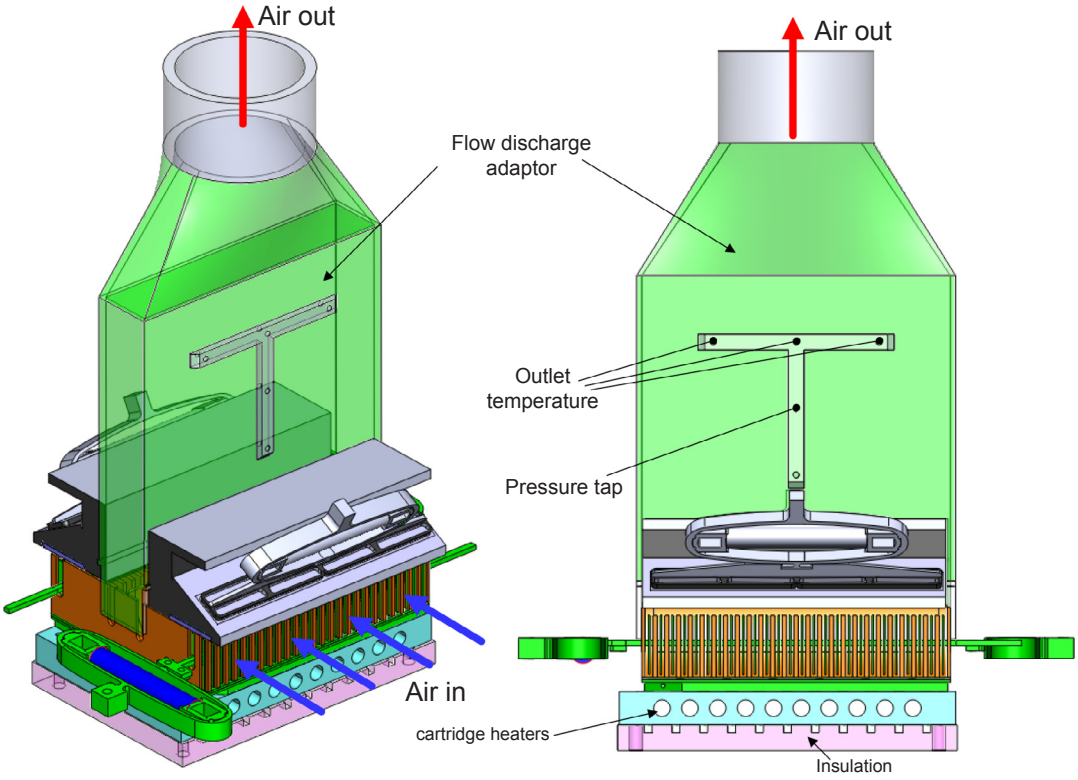

Fig. 8. Test section configuration with the active heat sink system.

$$R_{th} = (T_s - T_{in})/q$$

where T_s and T_{in}, and q are the average temperature of the heat sink base, the air inlet temperature, and the heat dissipation. The heat dissipation is calculated using an energy balance between the inlet and outlet as:

$$q = \dot{m} c_p (T_{out} - T_{in})$$

where $\dot{m}$, c_p, and T_{out} are the mass flow rate, specific heat, and air outlet temperature, respectively.

The system power consumption is calculated by summing the power consumption of each component with the addition of the fan power required to drive the flow though the heat sink:

$$P_{system} = P_{fan} + P_{agitator} + P_{jet}$$

The required suction power of the fan is computed by multiplying the pressure drop across the heat sink channels and volume flow rate with the 30% fan efficiency measured by a fan supplier. The fan power is:

$$P_{fan} = \frac{\Delta p \times Q}{\eta}$$

where Δp, Q, and η are the pressure drop, volumetric flow rate, and fan efficiency, respectively. The electrical power consumption values of the agitators and jets are calculated by measuring time-varying applied voltage (V(t)) and current (I(t)) to the agitator as:

$$P_{agitator} = \frac{1}{\tau} \int_0^t V(t) \cdot I(t) dt$$

where τ is the period of data measurement. Fig. 9 shows a schematic of the heat transfer experimental fixture. A vacuum pump is used instead of the actual suction fan to generate the channel flow through the active heat sink. A laminar flow meter is positioned between the test section and the blower to measure volume flow rates. A function generator and a voltage amplifier produce an amplified sine wave signal to drive the piezoelectric translational agitators and synthetic jets. A DC power supply is used to provide power to the heaters. Manometer measure the pressure drop across the heat sink and across the flow meter. An Agilent data acquisition system is used to obtain the temperature measurements. Fig. 10 shows the oscillating blades of the PTA2 agitator at the upstream of the channels. The operating frequency and displacement are 512 Hz and 1.4 mm, respectively.

The uncertainty in the thermal resistance measurement is propagated from the uncertainties in temperature measurements and volume flow rate measurements. The uncertainties in temperature and flow rate measurements are within 0.5 °C and 0.017 CFM (0.008 L/sec), respectively. Based on the propagation methodology of Moffat [41], the calculated uncertainty of the system thermal resistance measurement is 7%.

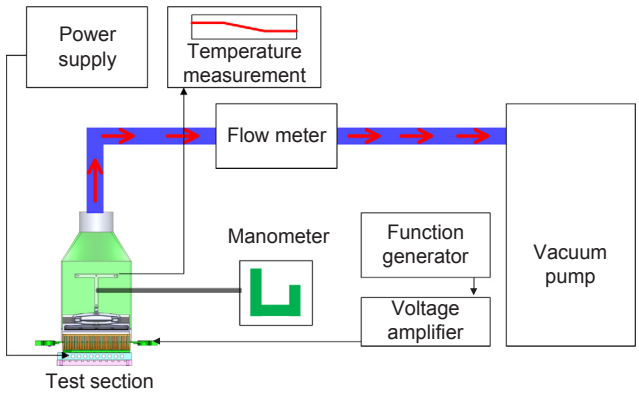

Fig. 9. Schematic of heat transfer experiment.

3.2. Experimental results

The thermal resistances of the active heat sink with either plain or micro pin-finned surfaces are presented at different volume flow rates and different operation conditions of the active components, as shown in Fig. 11. The specific target application of the current study is high power military computing platforms that consume and dissipate higher level of power compared to the commercially available computing systems. The range of the flow rate tested is between 56 CFM (26.4 L/sec) and 76.5 CFM (36.1 L/sec) which can be provided within the power budget allowed for the study. When only the throughflow of 56 CFM (26.4 L/sec) is applied to the plain surface heat sink and the active components are not energized, the thermal resistance of the system is 0.139 °C/W. When the agitator PTA-1 is turned on, the agitation at 222 Hz with the peak to peak displacement of 1.0 mm reduces the thermal resistance by 3.5% to 0.135 °C/W. This small enhancement in heat transfer is mainly due to the low operating frequency of the agitator. Once the PTA-3 is installed in the plain surface heat sink the thermal resistances are larger than those from non-activated PTA-1 case. The short blades of PTA-3 increase the flow path area of the channels, and reduce the flow velocity, resulting in larger thermal resistances. Generally, the existence of non-activated blades in the heat sink channels enhances heat transfer performance due to the increased flow velocity, however, this leads to the increase in pressure drop. These characteristics were evaluated in the component level study performed by Yeom et al. [42].

On the other hand, PTA-3 operating at about 800 Hz with 1.4 mm displacement reduces the thermal resistance by 18%–22%, depending on the flow rates. The comparison of heat transfer enhancement between PTA-1 and PTA-3 indicates that either or both the operating frequency and the displacement are key parameters that have significant impact on the performance of the agitator. The effect of the size of the blade is relatively minor. When the heat sink is replaced with one having micro pin fins, the system thermal resistance drops significantly by 31%–38%, without operation of agitators and jets. This exceeds those performed by PTA-3 at the same flow rates. Operation of the agitators over the micro pin fin heat sink further reduces the thermal resistance. The PTA-2 agitator operating at 512 Hz with 1.4 mm displacement achieved about a 10% reduction in thermal resistance compared to the non-agitated micro pin fin heat sinks. This is a total reduction of 44% (at 76.5 CFM or 36.1 L/sec) in thermal resistance from that of the non-agitated plain heat sink. PTA-3 shows slightly improved thermal performance at the lower flow rate of 63 CFM (29.7 L/sec). However, as the flow rate increases, it starts to converge to the performance of the PTA-2 agitator. The PTA-3 agitator operates at a higher frequency with the same displacement as the PTA-2 agitator. This shows that the displacement might be slightly more important than frequency in improving heat transfer performance of the active heat sink. On the other hand, when the jets are turned on, the thermal resistance drops only about 4.5% and 3.0% from those of non-agitated and agitated micro pin fin heat sink cases, respectively. The reason of the small contributions can be found from the specific configuration of the active heat sink in which the jets cover only a small fraction of heat transfer area, in the vicinity of fin tips, whereas the agitators provide direct impact on a large area of the fin side walls. Most interestingly, the superiority of the micro pin fins is clearly revealed from a comparison of two points in Figs. 11 and 12 between the non-agitated plain heat sink (Plain – PTA-3 Off) at 76.5 CFM (36.1 L/sec) and the non-agitated micro pin fin heat sink (Micro – PTA-2 Off) at 63 CFM (29.7 L/sec). The non-agitated plain heat sink achieves a thermal resistance of 0.119 °C/W at a power consumption of 32 W. On the other hand, the non-agitated micro pin fin heat sink at 63 CFM (29.7 L/sec) consumes less power, 27.4 W, while achieving a thermal resistance of 0.088 °C/W. The same comparison can be applied between the plain heat sink and micro pin fin heat sink for the cases with agitators turned on. The micro pin fin heat sink coupled with PTA-3 achieves a thermal resistance of

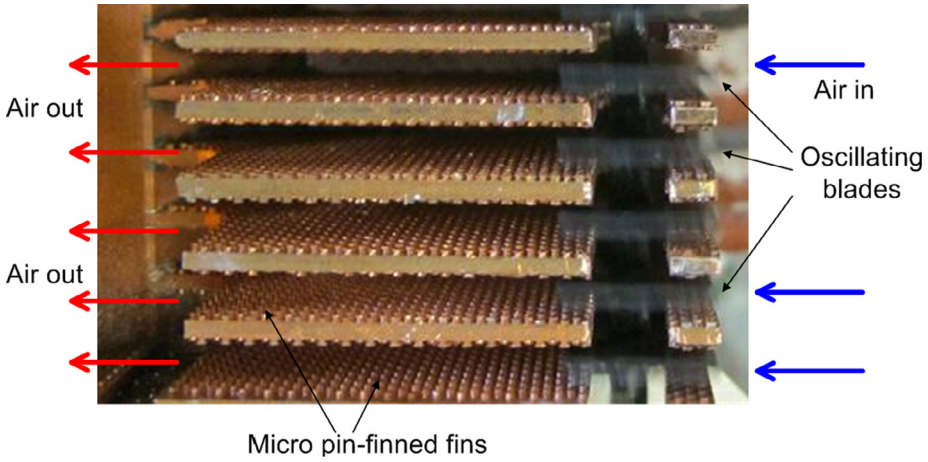

Fig. 10. Oscillating short-blade agitators in the heat sink channels with micro pin fins.

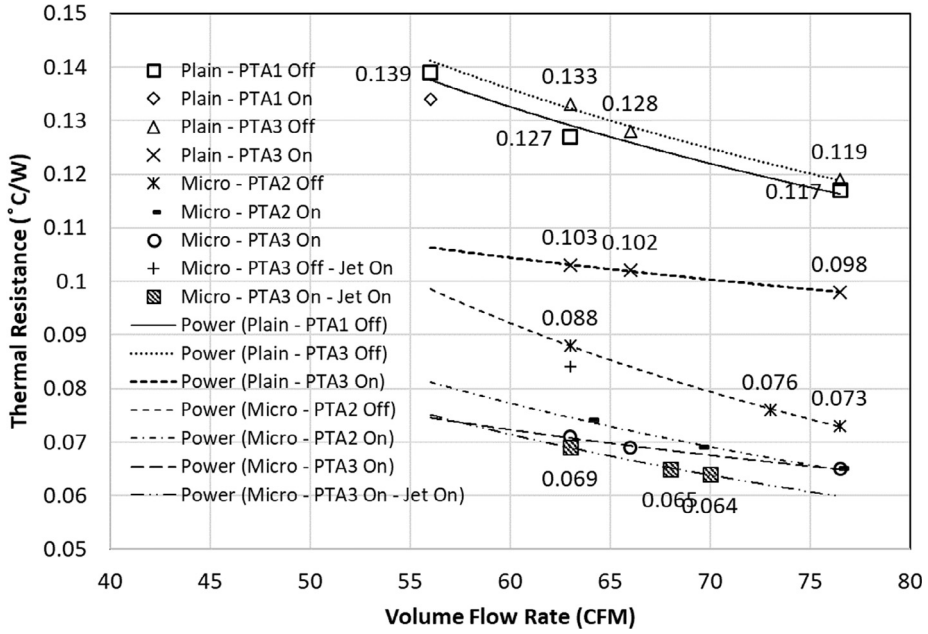

Fig. 11. System thermal resistance.

0.071 °C/W, while consuming about 43 W at 63 CFM (29.7 L/sec). This is a similar power consumption to that of the plain heat sink operating at 76.5 CFM (36.1 L/sec), which generates a thermal resistance of 0.119 °C/W. Finally, with the aid of all three components; agitator, jet, and micro pin fins, the active heat sink system achieves the thermal resistance of 0.064 °C/W at 70 CFM (33 L/sec), a 48% reduction from the non-agitated plain heat sink operating at the same flow rate and with 65.4 W of power consumption.

Fig. 13 shows the % contribution of each active and passive component in the active heat sink system to the total thermal resistance reduction. The % contribution is calculated by getting the reduction of thermal resistances when each cooling component is activated from the plain and non-agitated heat sink condition, and dividing them with the total thermal resistance reduction when all the cooling components are activated at each flow rate. The data points, which were not tested in the study, are estimated using the power curves displayed in Fig. 11. The bar chart confirms again that the micro pin fins have the largest contribution on the total thermal resistance at the entire range of flow rate tested. The synthetic jets show the least contribution on the total heat transfer enhancement. One interesting observation is that the effects of micro pin fins and synthetic jets increase as the flow rate increases whereas the agitators plays less role in reducing the thermal resistance as the flow rate increases. Further detailed studies on flow and temperature fields are required to fully uncover the underlying phenomena on this trend.

Noise is one of the important aspects for the cooling systems and has to be addressed especially for the systems utilizing piezoelectric components that can generate high level of acoustic noise. The acoustic noise characterizations of the active components used in the current study and the suggested noise reduction method are presented in the previous work conducted by Huang et al. [43]. According to the study, the A-weighted noise level of the current active heat sink system can reach as high as 100 dB and this can be reduced to the range of 60 dB utilizing the optimized expansion chamber.

4. Conclusions

An active heat sink system employing piezoelectric translational agitators, piezoelectric synthetic jets, and micro pin fins was introduced, and its thermal performance was experimentally validated. An oval loop shell coupled with a piezoelectric stack actuator was used to drive translational agitators and synthetic jets. Three different types

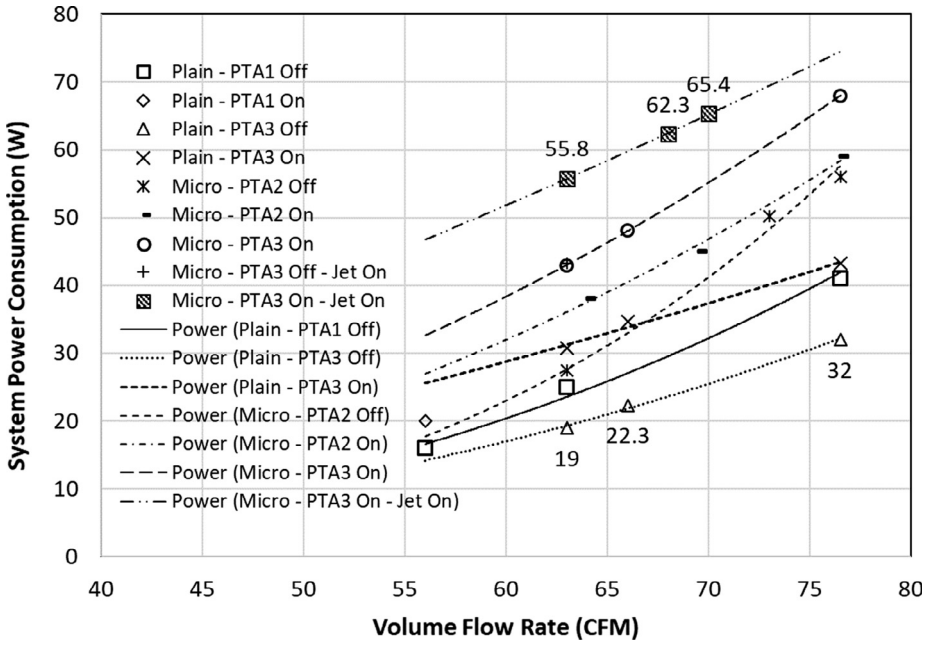

Fig. 12. System power consumption of the active heat sink system at operating conditions and various flow rates.

of carbon fiber blade structures were fabricated and used for the heat transfer experiments. For the synthetic jet, the wedge platform that enables inclined jet configurations was used to avoid any interference between the jet modules and the suction fan. Micro pin fins were electroplated on the copper substrate and cut into the heat sink fins. The heat transfer experimental results indicate that the micro pin fins are most valuable in reducing system thermal resistance and power consumption. The micro pin fins on the heat sink surfaces reduced thermal resistance by 38%, compared to the plain heat sink operated at the same flow rate. The micro pin fin heat sink combined with the PTA-3 agitator, operating at around 800 Hz and a displacement of 1.4 mm, generated a reduction of thermal resistance of 39% at 63 CFM (29.7 L/sec), while consuming a similar amount of power to that of the non-agitated plain heat sink with increased flow rate of 76.5 CFM (36.1 L/sec). These results indicate that the proposed active heat sink is a more efficient method than the traditional fan-assisted system with merely increased fan power to achieve the same level of cooling performance.

Conflict of interest

The authors declare that there is no conflict of interest.

Acknowledgements

This work was partially supported by the Defense Advanced Research Projects Agency (DARPA) MACE Program and the Minnesota Supercomputer Institute. The views expressed are those of the authors and do not reflect the official policy or position of the Department of Defense or the U.S. Government. Approved for Public Release, Distribution Unlimited.

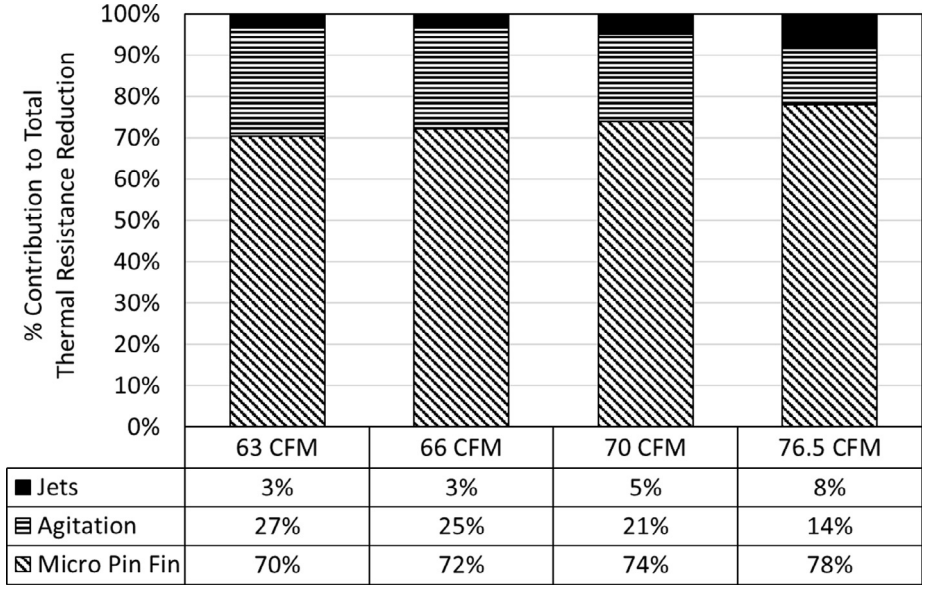

	63 CFM	66 CFM	70 CFM	76.5 CFM
Jets	3%	3%	5%	8%
Agitation	27%	25%	21%	14%
Micro Pin Fin	70%	72%	74%	78%

Fig. 13. Thermal resistance contribution of each active and passive cooling component at various flow rates.

References

[1] S.C. Mohapatra, D. Loikits, Advances in liquid coolant technologies for electronics cooling, in: Semiconductor Thermal Measurement and Management Symposium, 2005 IEEE Twenty First Annual IEEE San Jose, CA, USA, 2005, pp. 354–360.

[2] T. Salem, S.B. Bayne, D. Porschet, Y. Chen, Thermal performance of water-cooled heat sinks: a comparison of two different designs, in: Semiconductor Thermal Measurement and Management Symposium, 2005 IEEE Twenty First Annual IEEE San Jose, CA, USA, vol. 121, 2005, pp. 129–133.

[3] T.A. Shedd, A.G. Pautsch, Spray impingement cooling with single- and multiple-nozzle arrays. Part II: Visualization and empirical models, Int. J. Heat Mass Transf. 48 (15) (2005) 3176–3184.

[4] M. Fabbri, V.K. Dhir, Optimized heat transfer for high power electronic cooling using arrays of microjets, J. Heat Transf. 127 (7) (2004) 760–769.

[5] M. Fabbri, S. Jiang, V.K. Dhir, A comparative study of cooling of high power density electronics using sprays and microjets, J. Heat Transf. 127 (1) (2005) 38–48.

[6] M. Visaria, I. Mudawar, Theoretical and experimental study of the effects of spray inclination on two-phase spray cooling and critical heat flux, Int. J. Heat Mass Transf. 51 (9) (2008) 2398–2410.

[7] M. Visaria, I. Mudawar, Application of two-phase spray cooling for thermal management of electronic devices, IEEE Trans. Compon. Packag. Technol. 32 (4) (2009) 784–793.

[8] L. Jiang, M. Wong, Y. Zohar, Phase change in microchannel heat sinks with integrated temperature sensors, J. Microelectromech. Syst. 8 (4) (1999) 358–365.

[9] L. Jiang, M. Wong, Y. Zohar, Forced convection boiling in a microchannel heat sink, J. Microelectromech. Syst. 10 (1) (2001) 80–87.

[10] K.C. Marston, M. Gaynes, R.J. Bezama, E.G. Colgan, A practical implementation of silicon microchannel coolers, Electron. Cooling (2007).

[11] M. Arik, A. Bar-Cohen, S.M. You, Enhancement of pool boiling critical heat flux in dielectric liquids by microporous coatings, Int. J. Heat Mass Transf. 50 (5) (2007) 997–1009.

[12] N. Bakhru, J.H. Lienhard, Boiling from small cylinders, Int. J. Heat Mass Transf. 15 (11) (1972) 2011–2025.

[13] P.J. Berenson, Experiments on pool-boiling heat transfer, Int. J. Heat Mass Transf. 5 (10) (1962) 985–999.

[14] S.M. Kwark, R. Kumar, G. Moreno, J. Yoo, S.M. You, Pool boiling characteristics of low concentration nanofluids, Int. J. Heat Mass Transf. 53 (5) (2010) 972–981.

[15] P.J. Marto, V.J. Lepere, Pool boiling heat transfer from enhanced surfaces to dielectric fluids, J. Heat Transf. 104 (2) (1982) 292–299.

[16] K.-H. Sun, J.H. Lienhard, The peak pool boiling heat flux on horizontal cylinders, Int. J. Heat Mass Transf. 13 (9) (1970) 1425–1439.

[17] S.M. You, J.H. Kim, K.H. Kim, Effect of nanoparticles on critical heat flux of water in pool boiling heat transfer, Appl. Phys. Lett. 83 (16) (2003) 3374–3376.

[18] S.M. You, T. Simon, A. Bar-Cohen, A technique for enhancing boiling heat transfer with application to cooling of electronic equipment, IEEE Trans. Compon., Hybrids, Manuf. Technol. 15 (5) (1992) 823–831.

[19] M. Toda, S. Osaka, Vibrational fan using the piezoelectric polymer PVF2, Proc. IEEE 67 (8) (1979) 1171–1173.

[20] J.H. Yoo, J.I. Hong, W. Cao, Piezoelectric ceramic bimorph coupled to thin metal plate as cooling fan for electronic devices, Sens. Actuators, A 79 (1) (2000) 8–12.

[21] T. Açikalin, S.M. Wait, S.V. Garimella, A. Raman, Experimental investigation of the thermal performance of piezoelectric fans, Heat Transfer Eng. 25 (1) (2004) 4–14.

[22] S.M. Wait, S. Basak, S.V. Garimella, A. Raman, Piezoelectric fans using higher flexural modes for electronics cooling applications, IEEE Trans. Compon. Packag. Technol. 30 (1) (2007) 119–128.

[23] H.K. Ma, H.C. Su, C.L. Liu, W.H. Ho, Investigation of a piezoelectric fan embedded in a heat sink, Int. Commun. Heat Mass Transfer 39 (5) (2012) 603–609.

[24] S.F. Sufian, M.Z. Abdullah, Heat transfer enhancement of LEDs with a combination of piezoelectric fans and a heat sink, Microelectron. Reliability 68 (Supplement C) (2017) 39–50.

[25] T. Yeom, T.W. Simon, L. Huang, M.T. North, T. Cui, Piezoelectric translational agitation for enhancing forced-convection channel-flow heat transfer, Int. J. Heat Mass Transf. 55 (25) (2012) 7398–7409.

[26] N. Beratlis, M.K. Smith, Optimization of synthetic jet cooling for microelectronics applications [VCSEL array example], in: Ninteenth Annual IEEE Semiconductor Thermal Measurement and Management Symposium, 2003, 2003, pp. 66–73.

[27] R. Mahalingam, N. Rumigny, A. Glezer, Thermal management using synthetic jet ejectors, IEEE Trans. Compon. Packag. Technol. 27 (3) (2004) 439–444.

[28] M. Arik, Local heat transfer coefficients of a high-frequency synthetic jet during impingement cooling over flat surfaces, Heat Transfer Eng. 29 (9) (2008) 763–773.

[29] C. Marques, K.W. Kelly, Fabrication and performance of a pin fin micro heat exchanger, J. Heat Transf. 126 (3) (2004) 434–444.

[30] Y. Wang, F. Houshmand, D. Elcock, Y. Peles, Convective heat transfer and mixing enhancement in a microchannel with a pillar, Int. J. Heat Mass Transf. 62 (Supplement C) (2013) 553–561.

[31] A. Koşar, C. Mishra, Y. Peles, Laminar flow across a bank of low aspect ratio micro pin fins, J. Fluids Eng. 127 (3) (2005) 419–430.

[32] R.S. Prasher, J. Dirner, J.-Y. Chang, A. Myers, D. Chau, D. He, S. Prstic, Nusselt number and friction factor of staggered arrays of low aspect ratio micropin-fins under cross flow for water as fluid, J. Heat Transf. 129 (2) (2006) 141–153.

[33] M. Liu, D. Liu, S. Xu, Y. Chen, Experimental study on liquid flow and heat transfer in micro square pin fin heat sink, Int. J. Heat Mass Transf. 54 (25) (2011) 5602–5611.

[34] J.F. Tullius, T.K. Tullius, Y. Bayazitoglu, Optimization of short micro pin fins in minichannels, Int. J. Heat Mass Transf. 55 (15) (2012) 3921–3932.

[35] M. Koz, M.R. Ozdemir, A. Koşar, Parametric study on the effect of end walls on heat transfer and fluid flow across a micro pin-fin, Int. J. Therm. Sci. 50 (6) (2011) 1073–1084.

[36] T. Yeom, T. Simon, T. Zhang, M. Zhang, M. North, T. Cui, Enhanced heat transfer of heat sink channels with micro pin fin roughened walls, Int. J. Heat Mass Transf. 92 (2016) 617–627.

[37] T. Yeom, T.W. Simon, Y. Yu, M. Zhang, S. Agrawal, L. Huang, T. Zhang, M.T. North, T. Cui, An active heat sink system with piezoelectric translational agitators and micro pin fin arrays, in: 2012 ASME International Mechanical Engineering Congress and Exposition, Houston, TX, USA, 2012.

[38] T. Yeom, T.W. Simon, M. Zhang, M.T. North, T. Cui, Highfrequency, large displacement, and low power consumption piezoelectric translational actuator based on an oval loop shell, Sens. Actuators A: Phys. 176 (Supplement C) (2012) 99–109.

[39] T. Yeom, T.W. Simon, M. North, T. Cui, High-frequency translational agitation with micro pin-fin surfaces for enhancing heat transfer of forced convection, Int. J. Heat Mass Transf. 94 (2016) 354–365.

[40] A. Ayaskanta, L. Huang, T. Simon, T. Yeom, M. North, T. Cui, Heat transfer enhancement of a heat sink by inclined synthetic jets for electronics cooling, in: ASME Summer Heat Transfer Conference, Minneapolis, MN, USA, 2013.

[41] R.J. Moffat, Using uncertainty analysis in the planning of an experiment, J. Fluids Eng. 107 (2) (1985) 173–178.

[42] T. Yeom, T.W. Simon, T. Zhang, M.T. North, T. Cui, Convective heat transfer enhancement with micro pin-fin surfaces cooled by a piezoelectrically-driven translational agitator, in: 2012 ASME International Mechanical Engineering Congress and Exposition, Houston, TX, USA, 2012.

[43] L. Huang, T. Simon, M. Zhang, T. Yeom, M. North, T. Cui, Noise measurements and reduction for high-frequency vibrating devices in the application of cooling electronics, in: 2012 ASME International Mechanical Engineering Congress and Exposition, Houston, Texas, USA, 2012.